Journal of New Technology and Materials (JNTM)
J. New Technol. Mater.
Vol. 13, N°01 (2023)49-56

OEB Univ. Publish. Co.

Evaluation of residual stress on epoxy based coating using X-Ray and FEM-ANN methods

H. H. Jasim

Chemical Engineering Department, College of Engineering, Basrah University, Basrah, Iraq

Corresponding author: raidhani73@yahoo.com

Received date: Jan. 12, 2023; accepted date: Apr. 01, 2023

Abstract

In this paper, measure the residual stress in three types of epoxy coatings used as a lining for crude oil storage tank (pure, Novolac and reinforced by glass-flake) using X-ray method and then compared with that predicted values using finite element and artificial neural network methods. The effect of coatings thickness, volumetric shrinkage, coating viscosity and the curing temperatures are studied in details. The results shows that the pure epoxy has large values of residual stresses, while the Novolac epoxy have smallest values and the reinforced by glass-flake have intermediate values. Tests results demonstrate that the coats cured at high temperatures has high residual stresses compared to that cured at lower temperatures.

Keywords: Curing temperature; residual stress; volumetric shrinkage; x-ray method; glass-flakes

1. Introduction

Residual stresses in epoxy coatings can be develop from different bases of sources: intrinsic, thermal, volumetric changes and lattice mismatch [1]. The volumetric changes occur during the curing/crosslinking process or from shrinkage due to chemical reaction of base and hardener of epoxy and thermal expansion/contraction due to temperature changes [2]. The thermal contraction of the epoxy resin upon cooling from the reaction temperature has a great effect on the formation of residual stresses in epoxy coating. Due to the mismatch in coefficient of thermal expansion of the resin and a hardener material or additions such as filler, fibers and glass-flake the two materials base and hardener shrink with a different rate and thus introduce residual stresses. Also the differential cooling of the epoxy may lead to the formation of stress gradients in the epoxy resin, especially when the temperature range contains the glass transition temperature. The cure conditions includes the curing temperature and thickness of epoxy coatings is the major influences in the initiated of residual stresses [3]. Intrinsic residual stresses may occur due to the effect of defects such as air bubblies and gran boundary in coatings [4].

Various techniques including numerical and experimental method are employed for determining the residual strain or stress in coatings. Most of the experimental methods include the curvature method, Raman spectroscopy and the X-ray diffraction (XRD) [5]. Some of these methods are destructive and some are nondestructive. The X-ray diffraction technique used as non-destructive technique for the measuring of surface residual stresses. In the X-ray diffraction, the strain in the crystal lattice is measured and the associated residual stress is determined from the elastic constants assuming a linear elastic distortion of the crystal lattice plane [6].

Numerical approaches include finite element method (FEM) and artificial neural networks (ANN) have been widely used in the analysis of residual stresses. Finite element method is a practical method of dissolving problems in all parts of engineering structures and taken the influences of various factors on the mathematical models [7]. The use of finite element computational methods for prediction residual stresses induced in epoxy coating layer involve complex non-linear analyses, and can be biased by the various boundary conditions, a large computational time, inappropriate assumptions and modeling procedures [8].

ANN method is a computational models, basically consists of simple integrating input and output units called artificial neurons that can simulate the structural organization and can be modeling and predict relationships between different input parameters [9]. The operation of these elements is based upon the operation of neurons within the brain and gives ANN the ability to cope with relationships that are highly complex and non-linear. When supplied with sufficient training data, ANN model are capable of capturing intricate relationships between parameters and detecting subtle trends that other computational approaches not be able to achieve that [10].

Residual stress evolution in epoxy coatings has been a small area of researches. Kozo [11] shows that the polymeric coatings have a crack and blister as a result of induced residual stresses in the coating. Peter [12] reviews

the X-ray technique for measuring and estimation of residual stresses in coating and coating related systems. He shows that an X-ray technique is good techniques in application of measure residual stresses in coatings. Kishore [13] used finite element method for analysis of thermal residual stresses of epoxy coating on steel surface for two cases: A cantilever metal-polymer bi-layer beam and three-dimensionally constrained metal-epoxy cylinders. His results indicated that FEM is a good approach in analysis of coating system.

Aboubakar [14] used an axisymmetric model for computation and analysis of the residual stresses in the fiber/epoxy interface. Two cases are considered using an epoxy matrix with glass and carbon fibers respectively with a different volume of fiber. The results show that the stresses at interface are affected by residual thermal stresses particularly in the free edges. Cheng et al. [15] synthesized and studies the curing temperature and thermal stability of novel epoxy coatings contains the 4,4-diaminodiphenyl sulfone as hardener and the 4,4-diaminodiphenylmethane as base using differential scanning calorimetry. They found that the thermal decomposition temperature of epoxy coatings increased with the increase of curing time and rise the curing temperature. Hadjiev et al. [16] measure the residual stresses used Raman spectroscopy method in diglycidyl ether of bisphenol-F (DGEBF) epoxide systems. The used for cuing process the hardener diethyltoluenediamine (DETDA). They found that the residual stresses effect on strength properties of coatings. Frantisek et al. [17] developed a new approach using neural network method to analysis of residual stresses and compare their results with that obtained from experimental C-Ring measurement method. It has been shown that the neural network method is a good procedure to analysis of residual stresses. Taisei et al. [18] measure the residual stress in polyamide film polymer using X-ray diffraction method. They used a diffractormeter for measurement and show its good methods to apply in polymer coatings.

In this study, the evaluation and comparison of the residual stress of three different types of commercial Hampel epoxy coatings used for crude oil storage tanks of Basrah fields of south Iraq is achieved. The effect of coatings thickness, volumetric shrinkage, coating viscosity and curing temperature were studied in details. Finite element method has been adopted to generate the data set for artificial neural networks model to predict the equivalent residual stress within the epoxy coatings layer and then compared with experimental measurement using X-ray method.

2. Experimental and numerical procedures

2.1 Types of epoxy coatings

Three types of commercial epoxy coatings used for coating of crude oil storage tanks in south Iraq were used for studies. These coatings consist of two parts (base and hardener) which are in the liquid state and mixed together before applied coats on steel surface. These coatings are:

- HEMPADUR 15600, amine adducts cured pure epoxy coats. The mixing volume ratio is 1:1 of base to hardener. The thickness of coatings ranges 160-200 μm. Refer to this coat as model A.
- HEMPADUR 85671, this is a two component solvent free amine cured phenol Novolac epoxy coating. The volume ratio of mixing 1:2 of base epoxy to hardener. The thickness of this coating in the range 250 - 600μm. Refer to this type of coats as model B.
- HEMPADUR multi-strength GF-35870 is an amine-adduct cured epoxy coating, the coats is reinforced with glass-flakes. The mixing volume ratio is 3:1 of base to hardener. The maximum thickness of coatings is 350 μm. Refer to this type of coats as model C.

These types of Hampel epoxy coatings are manufacture by Sharjah coating company, U.A.E.

2.2 Specimen preparation and coats

The samples of (3*3) cm dimensions with thickness (6 mm) were used of ASTM A537 C1 carbon steel which was widely applied in building of crude oil storage tanks of south Iraq. The chemical compositions of ASTM A537 carbon steel as percentage are: Fe: 97.58, C: 0.24, Mn: 1.6, P: 0.035, S: 0.035, Cr: 0.025, Si: 0.5, Mo: 0.8, Ni: 0.25, Cu: 0.35 [19]. Figure 1 shows specimens before and after coats. The classes of Hampel coatings were applied by airless spray to steel substrates at nominally standard film thicknesses as given by manufactured company. To study the effect of curing temperature on the residual stresses induced during solidification, the samples of the three models of coatings were left to cure at nine temperature (10, 15, 20, 25, 30, 35, 40, 45 and 50°C) respectively. A total 100 specimens were used for X-ray measurement.

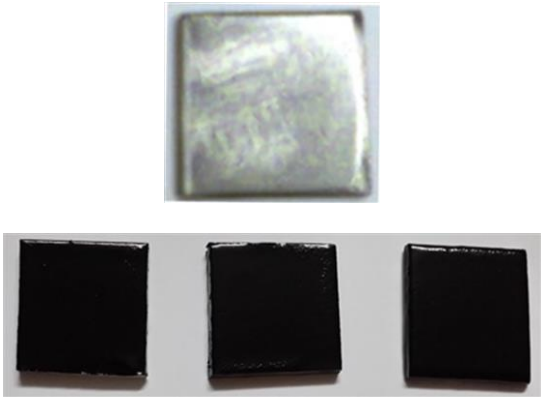

Model A Model B Model C

Figure 1. Specimens before and after coats.

2.3 Residual stress measured by X-Ray

In the method of X-ray diffraction (using the $\sin^2$ method) for measuring surface residual stress, the strains in the crystal lattice of coatings were measured along tangential direction and the associated residual stress is computed from the elastic constants (modulus of elasticity and Poison's ratio) [20]. The main assumption during measurement that the crystal lattice plane under appropriate linear elastic distortion. In the case of epoxy coatings, the penetration depth of X-ray is a small. The equations for residual stress computed from lattice measurement can be obtained by assuming a biaxial state of stress. The d-spacing's are measured using diffractometer for a different values of Ψ and the residual stress is calculated by using the following relation [21]:

$$\sigma_{res.} = \frac{E}{(1+\nu)\sin^2(\psi)} \frac{d_n - d_o}{d_o} \quad (1)$$

The X-ray measurements were performed on a ADX-8000 Mini θ-θ Powder X-ray diffraction instrument manufactures by Angstrom Advanced Inc. The X-ray source is cu tube which is used for all specimen tested. The X-ray energy used for measuring residual stress is comparatively low (10 kV). Since the thickness of epoxy coats is relatively small and only the surface strain can be achieved. The goniometer used to read and record the angle (2θ). The Collimator used to control the irradiated area. Table 1 listed the specification used by X-ray diffraction. Figure 2 shows the method of measuring residual strain.

The residual stress calculation from Eq.(1) needs to know the unstressed lattice spacing do, the stressed lattice spacing d_n, the elastic modulus and the Poisson's ratio of coatings. Various methods are found to obtain unstressed lattice spacing. The (ω) is the angle between the incident X-ray beam and sample surface is half of (2θ). In this paper the value of lattice spacing measured at ψ = 0 is consider do. The diffraction angle (2θ) is measured directly during experiment test. Then from the diffraction angle, the stressed lattice spacing d_n is calculated, and the known X-ray wavelength using Bragg's law [22], i.e., the stressed lattice spacing d_n is obtained from drown a curve the intensity versus scattering angle (2θ) obtains from X-ray measurement. The stressed lattice spacing d_n is the peak intensity in this curve. The values of elasticity modulus and Poison's ratio obtained from tensile test.

The measurement of mechanical properties (elastic modulus (E) and Poison's ratio (ν)) of the epoxy coating has some difficulties, because the structure of epoxy coatings is complex and contains lamella, pores, micro cracks and so on. This, Poison's ratio and modulus of elasticity of the epoxy coatings was determined using the tensile test. The Hounsfield hand operated universal tensile testing machine SM1002, Hounsfield Company, UK) accordance to ASTM E8M-01[23] and ASTM D638-14 [24] were used for achieving tensile test to measure elastic modulus and Poisson's ratio of the three types of epoxy coatings. Two strain gage were used one to measure longitudinal deformation and the other to measure contraction in median of specimen during test.

Table 1: List of specifications of X-ray diffraction.

Specification	Values
Chart speed	15 mm/min
Incident angle of X-ray	0,18,36,45
Gonio scan speed	1 deg/min.
Divergent angle	0.35 deg.
Irradiation area	3*3 mm^2
Time constant	5 Sec
Tube current	15 mA

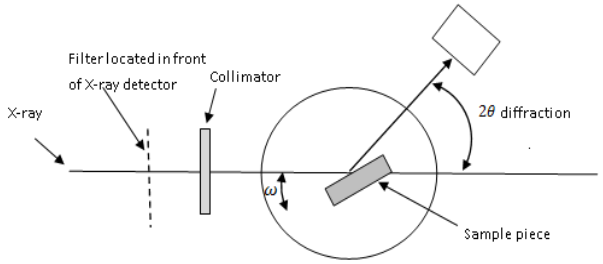

Figure 2. Method of measuring residual stress using X-ray method.

Figure 3 shows specimen after mounding in molds and solidification. Using two glass plates have dimensions and shape similar to tensile test specimen given by ASTM E8M-01and ASTM D638-10 [23, 24] as mold for casting the three Hample epoxy coating to prepare the tensile specimens. Rubber bounding around the glass plates was used to fixing it. The specimens were left to cure at temperatures (10, 15, 20, 25, 30, 35, 40, 45 and 50 °C). The specimen has 50 mm gage length and 5 mmm diameter. The specimens are treated as elastic materials for tensile test. Total 54 specimens were prepared for tensile testing.

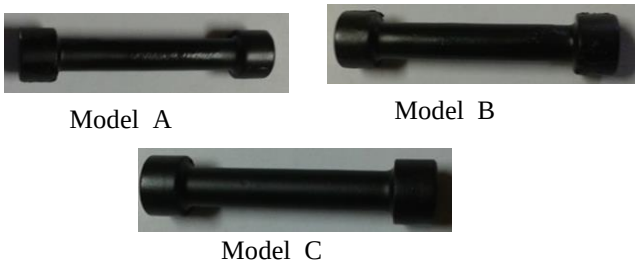

Figure 3. Tensile test specimen of the three types of epoxy coatings.

2.4 Finite element method (FEM)

Finite element method (FEM) was carried out using the commercial software ANSYS V.7 for both thermal and displacements analysis. The coatings were modeled in 3D

with 8-node quadratic quadrilateral elements. The meshes used in the models are shown in Fig.4. The boundary conditions for the models, that all nodes on top surface are subjected to temperature (10, 15, 20, 25, 30, 35, 40, 45 and 50°C) while bottom surface nodes are constrained in the X-Y directions.

The finite element analyses were carried out on 3D models using temperature-dependent material properties elastic modulus and poison's ratio. The elastic modulus and Poison's ratio are determined from tensile test specimens curing at various temperatures. The reference coefficient of thermal expansion (CTE) is $70*10^{-6}$/ °C for amine cured phenol Novolac epoxy, while for amine adduct cured pure epoxy paint is about $121.4*10^{-6}$ / °C and for amine-adduct cured epoxy coating reinforced with glass-flakes is about $30*10^{-6}$ /°C at room temperature according to company manufacturing data sheet information. For other temperatures, the coefficient of thermal expansion using in ANSYS V.7 software program is calculating using equation [25]:

$$\alpha_T = \frac{\ln(\alpha_{ref}*(T-T_{ref})+1)}{(T-T_{ref})} \quad (2)$$

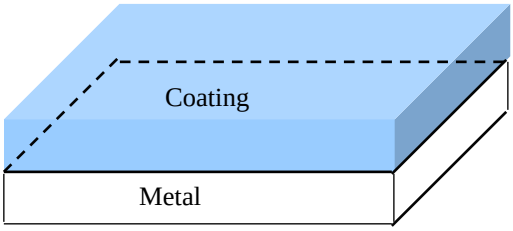

(a)

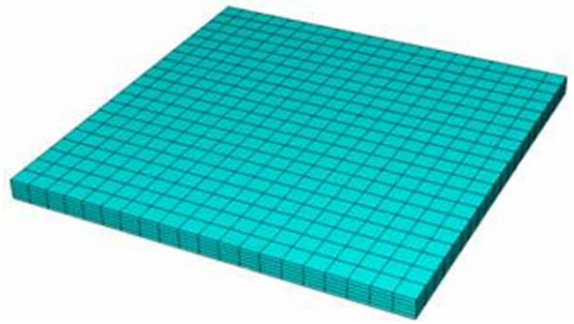

(b)

Figure 4. (a) Coating system (b) Finite element mesh for coatings.

2.4 Artificial neural network method (ANN)

For the predict analysis using ANN, the model ANN consists of three layers; the input layer, the hidden layer, and the output layer. The input parameters to the ANN model consist of the strains and displacement obtained from the numerical simulations using FEM with mechanical properties obtained from tensile test and the outputs are the corresponding residual stress predicted. The learning function is gradient descent algorithm with momentum weight and bias learning functions. The number of hidden layer and neurons are determined through a trial and error method in order to accommodate the convergence error. The structure of the proposed ANN model is 6 neurons in the input layer, 12 neurons in first hidden layer and 13 neurons in the second hidden layer and 1 neuron in the output layer. With a learning rate of 0.55 and momentum term 0.9. The network training is 10000 iterations. The error between the desired and actual output is less than 0.001at the end of the training process. Figure 5 show the basic architecture of artificial neural network model. The MATLAB R2010b, neural network toolbox was used during studies for training and testing data obtained from FEM and tensile test.

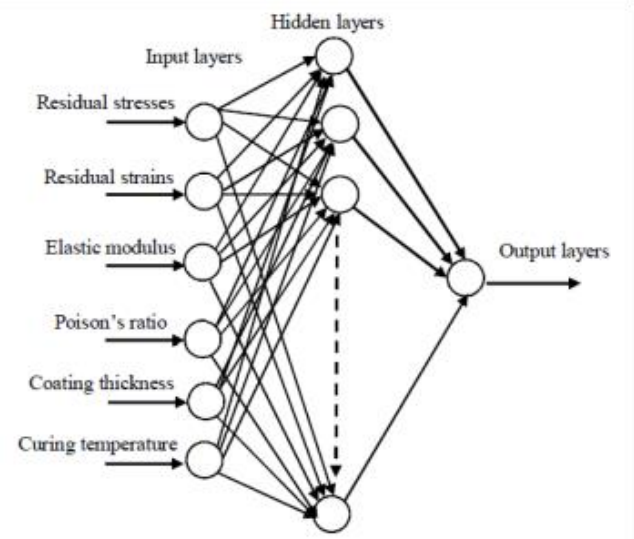

Figure 5. ANN architecture for residual stress prediction.

3. Results and dissuasion

Figure 6, show stress-strain curves of the three Hample epoxy coating cured at 10°C obtained from tensile test. As illustrated in Figure 6, there is linearly elastic response of the stress-strain curves until point of maximum stress followed by abrupt failure at strain larger 2.28 %, 2.47% and 2.68 % for models A, B and C respectively. Elastic modulus was extracted from stress-strain curves of Hample epoxy specimens curried at various temperatures, while Poison's ratio are determined from longitudinal and lateral strain measured by strain gages during test. The behavior of the three epoxy coating is similar metallic materials as indicated in all stress-strain curves, i.e. the tensile strength increased with increasing load until failure. Table 2 and 3 are summarized the elastic modulus and Poison's ratio for different cure temperatures.

As indicated from Tables 2 and 3, model C has lower values of elastic modulus and Poison's ratio due its rigidity because of reinforcement by glass-flake compared to others. Also the effect of increasing curing temperature in elastic modulus values is less compared to other types of coatings. For model A and B, the values of elastic modulus of elasticity have high effected by curing temperature and the modulus reduces as curing temperature increases. The effect of curing temperature on values of poison's ratio is very small compared to the effect on the values of elastic modulus.

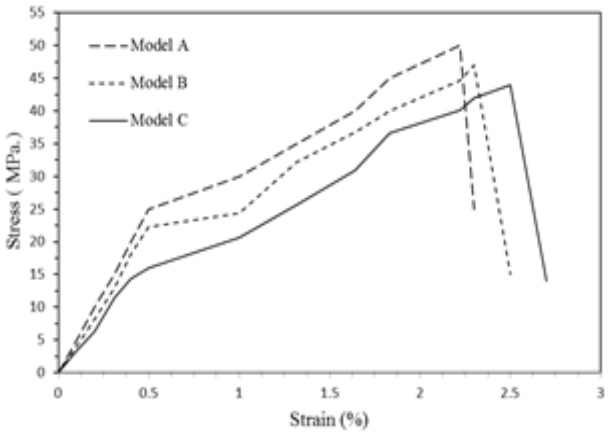

Figure 6. The stress-strain curve of the three types of epoxy coating cured at 10°C.

The displacements and strains in each element of the coating surface system is obtained by solving the n independent equations resulting from FEM meshes in three dimensions case. Then putting the results in ANN model to train it and calculating the residual stresses. In the finite element analysis, the boundary temperatures will set at curing temperature 10°C and then increase by step increment of 5°C for each case of calculation displacement and strains. Figure 7 compares the residual stresses of the three types of epoxy coatings cure at 10°C as a function of coating thickness. Also it compare between those measured using x-ray method at the center of coated specimen and those calculated by FEM-ANN method at room temperature. As indicated, the results appear to be in excellent agreement. The residual stresses in radial direction are very small so it's neglected and the stresses in tangential direction are considered only.

The maximum residual stresses for epoxy coatings obtained from the X-ray measurements are -20.9, -9.11 and -14.04 MPa for coatings A, B and C respectively. While that obtained from FEM-ANN method are -19.57, -8.72 and -13.61 MPa for coatings A, B and C respectively. The magnitude of the residual stresses is lower at the interface region of samples and began to increase with coating thickness increases. The increase coating thickness increase time needs to cure the coatings and this lead to increase reactions between base and hardener to form crosslink density of epoxy coatings. This lead to increase the values induced of stresses. Also it can be noted that the residual stresses distribution induced in a coating layer is not uniform through thickness and various due to different types of compositions and reinforcement. Also it can be noted that all residual stresses are compressive stresses. As seen the compressive residual stress would be produced because the reaction between base and hardener during mixing to produce epoxy coating was completely occurs after coating applied. Also the residual stress in the epoxy coating is compressive due to the smaller coefficient of thermal of the epoxy coat than that of the substrate of steel coated.

Table 2: Epoxy coating elastic modulus obtained from tensile test.

Cure temperature (°C)	Elastic modulus (GPa)		
	Model A	Model B	Model C
10	2.24	1.65	0.96
15	2.20	1.61	0.95
20	2.18	1.60	0.94
25	2.15	1.59	0.91
30	2.14	1.57	0.89
35	2.12	1.55	0.88
40	2.11	1.52	0.85
45	2.10	1.51	0.84
50	2.10	1.50	0.83

Table 3: Epoxy coating Poison's ratio obtained from tensile test.

Cure temperature (°C)	Poison's ratio		
	Model A	Model B	Model C
10	0.42	0.31	0.27
15	0.42	0.31	0.27
20	0.43	0.34	0.28
25	0.43	0.34	0.28
30	0.40	0.34	0.28
35	0.40	0.35	0.28
40	0.45	0.35	0.28
45	0.45	0.35	0.29
50	0.45	0.35	0.29

Model A consists from amine adduct cured pure epoxy paint have a high order of residual solvents, monomers, and low molecular weight extractible that have high residual stress induced compared to models B and C. Model C reinforced by glass-flak and this reduces the internal stresses induced.

Figure 8 shows the values of residual stresses obtained from X-ray measurement and FEM-ANN method as function of cure temperatures. Nine cure temperatures were chosen for studying, from 10°C to 50°C by increasing

cure temperature step of 5°C. As is evident from the Fig.8, the residual stress values significantly affected by temperature of solidification of epoxy coating. If the temperature is 10°C, the stress values are -12.98, -3.3 and -6.11 MPa for models A, B and C respectively. If the curing temperature is 50°C, the values of the residual stresses are -26.1, -17.6 and -21.3 MPa for models A, B and C respectively. This clear that there is a significant increase in residual stress values with increase of curing temperatures of epoxy coatings, while these values are lower in minor temperature. It found that the best temperature for hardening is 20°C which give lower values of residual stresses induced.

In case of amine adduct cured pure epoxy coating, if the curing temperature is low leads to low reactivity of the amine group when mixing process of amine hardener with epoxy. This causes an excess epoxy ring in the backbone and causes a fluctuation in the cuing rate or solidification rate of coatings, therefore, makes the cure mechanism difficult. This process induced high residual stress compared to other types. But the high curing temperature may be accelerated the reactivity of amine hardeners and reducing the time of solidification. In other word, increasing cure temperatures increase the evaporation of hardener (exothermic reactions or increase activation energy between base and hardener) which leads to increase the values of residual stresses induced. Also if the thickeners of the coating increased and the curing temperature rises, this make the coatings soft and become more flexible due to the escape or leak the heat could not be so easily. Thus increases in residual stresses with thickness of coatings.

One of the most important property of epoxy coats influences by curing temperature is the cross linking density of the epoxy coats and its process and this effected directly on the values of residual stress initiated. A very dense cross-linked between coating components form a very strong network through the epoxy coating and enhances its mechanical properties. In the case of model B contains Novolac coats. The Novolac epoxy coating results from the reaction of phenol function group (hardener) and formaldehyde resin (base). This after mixing process the curing process very cross-linked material can be gained. During cure, the cross link density of Novolac epoxy coating increases gradually, transforming the liquid reactants to a solid to yield amorphous solid. As the physical state of the Novolac coating changes during cure, it experiences residual stresses due to volume shrinkage and due to the effect of cured temperature.

For model C as the cured temperature rises, thermal expansion causes a decrease in tension on the glass-flake and increase compression of epoxy matrix. Due to the difference in the coefficient of expansion between glass-flake and epoxy matrix, this make residual stresses induced is rather small compared to model A. This for coating C, the coatings have medium values of compressive residual stresses but it's has high densities compared to the other types of coatings. In the other hand, in the glass flak/epoxy systems, a residual stress is developed during the thermal cure due to shrinkage of the epoxy. The cure shrinkage between glass-flake and epoxy base is less at lower curing temperature compared to elevate, this also lead to increase crosslink density results reduces stresses initiated. But the shrinkage due to chemical curing and crosslinking of the Novolacs epoxy is larger than that of models C coats.

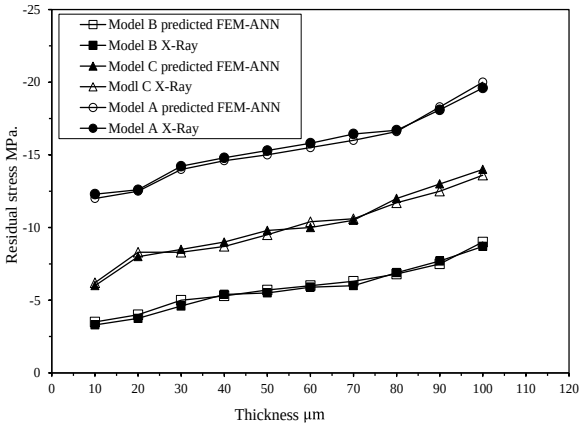

Figure 7. Residual stress vs. thickness for three epoxy coatings cure at 10°C.

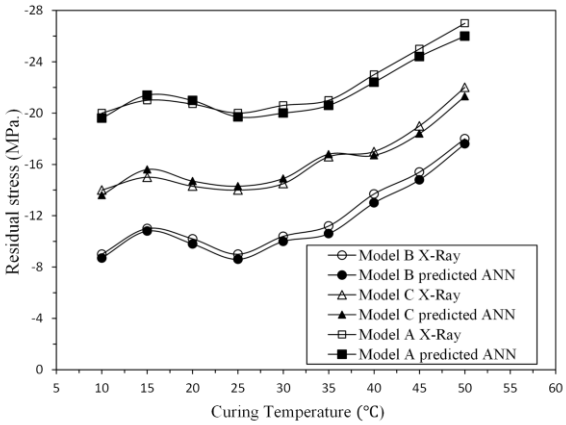

Figure 8. Residual stress vs. curing temperatures for the three types of epoxy coatings.

To make comparison between the volumetric shrinkage of tested epoxy coatings, the volumetric shrinkage of the three epoxy coats was calculated using the equation [26, 27]:

$$\text{Volumetric shrinkage [\%]} = 1 - \frac{\rho_u}{\rho_c} * 100\ \% \qquad (3)$$

The density of curing epoxy coats were determined experimentally using simple method on a cylindrical specimen, a cavity is made on specimen following for which the epoxy coats is sprayed on it. After spraying the coating ground to make this specimen cylindrical. Given the size known of substrate, the volume of the coating can then be calculated. After the specimens is grinding and weighted the coats grind to obtain the mass of coating [28].

Table 4, show the density of uncured epoxy coats which given by data sheets of manufactures company [29, 30, 31] and those calculated by using direction method for curing epoxy coats.

The values of volumetric shrinkage calculated for the three models are 5.10 %, 3.73 % and 4.55 % for models A, B and C respectively. The model A contain amine adduct pure epoxy coatings show large volume shrinkage upon curing, while model B show low shrinkage upon curing process, model C show moderate value.

The reinforcement occupy small position in epoxy coats and formed from local shrinkage during curing of the epoxy and hardener reactions and act as a bridge interconnecting coatings molecules. This result shows reduced volume shrinkage in addition to an increase the cross-linking density [32]. The formation of voids in the cured amine adduct pure epoxy coats is occurs due to the volume shrinkage during the curing reaction, and thus results in increasing the inducing internal stresses in this coats [33]. The volume shrinkage has been conventionally reduced by the addition of organic and inorganic reinforcement. However, addition of reinforcement to curable composition frequently results in an increase in viscosity and thus reduces fluidity [34, 35].

Table 4: The density of uncured and cured epoxy coats of the three models.

Uncured and cured coats	Density (kg/m^3)		
	Model A	Model B	Model C
Uncured epoxy coats	1600	1700	1300
Curing epoxy coats	1686	1766	1362

At low temperatures, the base-hardener epoxy coating cure reaction preceded very slowly comparison to that at high temperature and this effect on the values of stresses initiated. At 20°C the reaction becomes stable compared to other temperature and this lead to make the residual stresses initiated is small compared to other curing temperatures. The results show that the tangential residual stress at high curing temperature is higher for the three models of epoxy coat when it is compared to lower curing temperature.

Novolac curing epoxy coating is larger viscosity than the amine adducts curing epoxy. This the amine adduct curing epoxy has a lower reactivity when mixing epoxy resin with hardeners and this reduces curing process of these coats [36]. This high viscosity of Novolac epoxy coating make their curing process has very high functionality results in a very tight crosslink density compared to amine cure pure epoxy coat [37]. As curing process is low with time means initiation of residual stress increase with time increases. Adding glass-flake to model C increase the crosslink density, but also has been found to be increases in the residual stress compared to model B.

4. Conclusions

The influence of different cure conditions and thickness of epoxy coatings on values of residual stress was examined. From pervious discussion the following conclusion are recorded:

1- Good agreement obtained between X-ray method and FEM-ANN model.

2- The values of residual stresses influences by curing temperature change and the curing at low temperature can reduce residual thermal stresses compared to high temperatures.

3-All the residual stresses measured and calculated using FEM-ANN models of three types of epoxy coatings are compressive stresses.

4- The residual stresses are varies throughout of coating thickness.

5-Model B contains free amine cured phenol Novolac epoxy has lower values of residual stresses while model A contains amine adduct cured pure epoxy has high values. Model C which reinforced by glass-flake has moderate values of residual stress.

Acknowledgement

The author thanks the stuffs at material science department, college of engineering, Baghdad University for help to achieve X-ray measurements.

References

[1] J. M. Arthur, R. W. Thomas, K. Jagannadham, Advances in X-ray Analysis, 41 (1999) 443-454.

[2] R. P. Anthony, Ph. D. Thesis, University of Massachusetts, USA , 2013.

[3] V. Antonucci, A. Cusano, M. Giordano, J. Nasser, L. Nicolais, Composites, 37 (2006) 592-601.

[4] H. Windischamann, G. F. Epps, Y. Cong, R. W. Collins, J. Appl. Phys., 69 (1991) 2231-2237.

[5] F. Yongqing, D. Hejun, Q. S. Chang, Thin Solid Films, 424 (2003) 107–114.

[6] M. E. Fitzpatrick, A.T. Fry, P. Holdway, F. A. Kandil, J. Shackleton, L. Suominen, Measurement Good Practice Guide No. 52, Report of national physics laboratory (NPL), UK, 2005.

[7] H. Mohammad, Mechanical and Mechatronics Engineering, 2 (2015) 93-104.

[8] J. Mathew, R. J. Moat, S. Paddea, M. E. Fitzpatrick , Bouchard P. J., International Journal of Pressure Vessels and Piping, 150 (2017) 89-95.

[9] D. Umbrello, G. Ambrogio, L. Filice, R. A. Shivpuri, Materls and Design, 29 (2008) 873-883.

[10] B. T. Thumati, J. Sarangapani, Recent Advances in Intelligent Control Systems, 1st. Edition, Springer, London, 2009.

[11] S. Kozo, Progress in Organic Coating, 8(1980) 143-160.
[12] K. J. Peter, Progress in Organic Coatings, 8 (2) (1980) 8-107.
[13] I. Kishore, MIE 605 Term Project, University of Massachusetts, USA, 2003.
[14] S. B. Aboubakar, Material Research, 12 (2009) 133-137.
[15] J. Cheng, J. Li, J. Y. Zhang, Express Polymer Letters, l (2009) 501–509.
[16] V. G. Hadjiev, G. L. Warren, L. Sun, D. C. Davis, D. C. Lagoudas, H. J. Sue, Carbon, 48 (2010) 1750-1756.
[17] M. Frantisek, M. Marcel, C. G. P. Cardona, F. G. Tabres, Applied Mechanics and Material, 11 (2014) 436-440.
[18] D. Taisei, N. Masyuki, O. Juinchi, Advance Material Research, 1110 (2015) 100-103.
[19] D. Gandy, Plate Specification Guide 2012-2013, Carbon Steel Handbook, USA, 2007.
[20] A. Osman, MSc. Thesis, Mechanical department, Texas A & M University, USA, 2004.
[21] P. G. Charles, Report of Army Material and Mechanical Research Center, MS83-1, Massachusetts, USA, (1983)1-49.
[22] C. Suryanarayana, M. Norton, Springer New York, NY, Plenum Press, USA, 1998, 237-249.
[23] C. Jennifer, E8/E8M-09, Standard test methods for tension testing of metallic materials, ASTM International Report, USA, 2000.
[24] C. Jennifer, ASTM D638-14, ASTM International Report, USA, (2015).
[25] X. Cheng, Support ANSYS Tips & Tricks, Report of Simu. Tech. Group, USA, 2015.
[26] C. Jennifer, ASTM D2566, Test method for linear shrinkage of cured thermosetting casting resins during cure, ASTM International Report, USA, 2012.
[27] N. Yasir, S. Salma, B. Nicolas, J. Frederic, J. of Mat. Sci., 48 (2013) 5387–5409.
[28] K. Magniez, A. Vijayan, N. Finn, Polymer Engineering and Science, 52 (2012) 346-351.
[29] C. Alun, HEMPADUR 15600 product data sheet, Annual Report Hample Coating Company, U.A.E., 2018.
[30] C. Alun, HEMPADUR 85671 Product data sheet, Annual Report Hample Coating Company, U.A.E., 2018.
[31] C. Alun, HEMPADUR MULTI-Strength GF 35870 product data sheet, Annual Report Hample Coating Company, U.A.E. 2018.
[32] J. Ramos, N. Pagani, C. Riccardi, J. Borrajo, S. Goyanes, I. Mondragon, Polymer, 46 (2005) 3323–3328.
[33] Y. Mei, Ph.D. Thesis, Rackham School of Graduate Studies, University of Michigan, Ann Arbor, Michigan, USA, 2000.
[34] S. Song, K.W. Shahwan, A. M. Waas, O. Faruque , X. Xiao, Composite Sci. Technol., 67 (2007) 3059-3070.
[35] L. Chun, Ph.D. Thesis, School of Materials, Faculty of Science and Engineering, University of Manchester, USA, 2017.
[36] D. W. Eric, R. W. Scott, Report of Army Research Laboratory, Aberdeen Proving Ground, MD 21005-5069, Russian, 2004.
[37] S. Chang, M.Sc. Thesis, Materials Science and Engineering Department, Virginia Polytechnic Institute and State University, USA, 2015.